Vortices in vibrated granular rods

Daniel L. Blair, T. Neicu, and A. Kudrolli
Department of Physics, Clark University, Worcester, Massachusetts 01610
(Received 19 February 2002; published 31 March 2003)

We report the experimental observation of vortex patterns in vertically vibrated granular rods. Above a critical packing fraction, moving ordered domains of nearly vertical rods spontaneously form and coexist with horizontal rods. The domains of vertical rods coarsen in time to form large vortices. We investigate the conditions under which the vortices occur by varying the number of rods, vibration amplitude, and frequency. The size of the vortices increases with the number of rods. We characterize the growth of the ordered domains by measuring the area fraction of the ordered regions as a function of time. A *void-filling* model is presented to describe the nucleation and growth of the vertical domains. We track the ends of the vertical rods and obtain the velocity fields of the vortices. The rotation speed of the rods is observed to depend on the vibration velocity of the container and on the packing. To investigate the impact of the direction of driving on the observed phenomena, we performed experiments with the container vibrated horizontally. Although vertical domains form, vortices are not observed. We therefore argue that the motion is generated due to the interaction of the inclination of the rods with the bottom of a vertically vibrated container. We also perform simple experiments with a single row of rods in an annulus. These experiments directly demonstrate that the rod motion is generated when the rods are inclined from the vertical, and is always in the direction of the inclination.

DOI: 10.1103/PhysRevE.67.031303 PACS number(s): 45.70.Ht, 45.70.Qj, 83.80.Fg

I. INTRODUCTION

Granular materials are well known examples of dissipative nonequilibrium systems that show a rich variety of collective phenomenon, such as convection, wave patterns, and segregation [1–4]. Most studies utilize spherical particles to investigate these bulk properties. However, in most natural or industrial settings one can find an abundance of anisotropic granular materials, viz., rice, medicine capsules, and even logs. Therefore it is surprising that very few studies of prolate granular materials have been carried out. Mounfield and Edwards [5] applied the concepts of configurational statistical mechanics to study the nature of the isotropic to nematic phase transition in a granular system of elongated particles. In recent experiments utilizing a tall narrow cylinder, Villarruel *et al.* [6] studied the effects of anisotropy on granular packing. They observed the appearance of smectic states with the direction given by the container walls.

In thermal systems, particle anisotropy is known to produce ordered states. Examples are rod and plate shaped colloids and liquid crystals, which show orientational order and form nematic and smectic phases [7–11]. The ordering mechanism was found to be entropically driven, i.e., as thermodynamic equilibrium is reached, the process of entropy maximization leads to long range order. It is not obvious that such mechanisms carry over to granular systems because the thermal energy scale is very much smaller than the potential energy required for particle rearrangement, and energy has to be supplied actively to produce sustained motion. Therefore, an interesting question arises—does shape anistropy lead to self-organization and pattern formation in granular materials?

In this paper we report the observation of vortex patterns exhibited by granular rods that are vibrated vertically inside a container. We obtain the phase diagram for the observed patterns as a function of the acceleration of the driving and the packing fraction of the rods. We find that for sufficiently large packing fractions, the rods tend to align vertically and undergo vortex motion. Using high frame rate imaging and particle tracking, we have measured the velocity fields of the vortices as a function of packing fraction and driving frequency. Based on our experimental observations, we argue that the inclination of the rods causes motion due to collisions with the bottom boundary. To bolster our claim, we conduct experiments with a single row of rods in an annulus to demonstrate that motion is always in the direction of inclination. Thus we show that shape anisotropy leads to translational motion in such systems.

II. EXPERIMENTAL APPARATUS

The experiments were performed in a circular anodized aluminum container with a diameter $D=6.0$ cm and depth $H=1.5$ cm. (Limited experiments were also carried out in a container with $D=8.5$ cm.) The container is leveled to within 0.002 cm and is attached to an electromechanical shaker through a rigid linear bearing that allows motion only in the vertical direction. The cell is driven by a sinusoidal signal at a frequency f, and is monitored by an accelerometer via a lock-in amplifier. The experiments were conducted using copper cylinders with uniform length $l=6.2$ mm and diameter $d=0.5$ mm. The cylindrical surface of the rods is coated with a gray tin-oxide layer to diminish light reflection and has a coefficient of friction $\mu=0.32$. The patterns that form are imaged from above using a high-frame rate digital camera (Kodak SR-1000). Since the flat ends of the rods reflect light better than the sides, they appear as bright spots when imaged from above. If the rods are inclined greater than 35°, they reflect far less light compared to nearly vertical and horizontal rods.

One control parameter for our experiments is $\Gamma=\mathcal{A}(2\pi f)^2/g$, where $\mathcal{A}$ is the driving amplitude and g is the

 ©2003 The American Physical Society

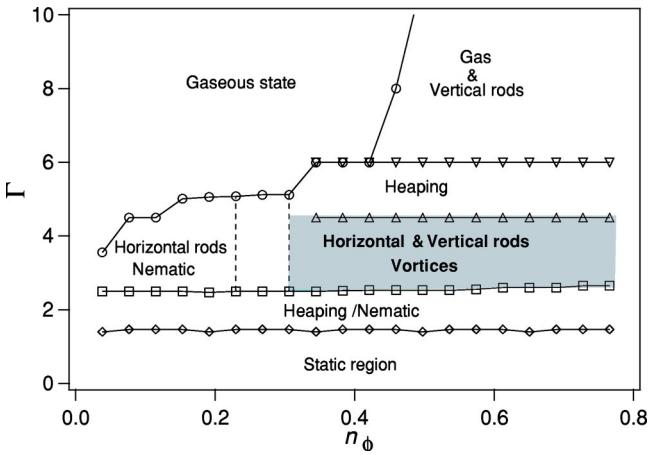

FIG. 1. (Color online) The phase diagram of the observed patterns in vibrated granular rods. The driving frequency $f=50$ Hz. Vortices are observed for sufficiently large numbers of rods and driving acceleration parameter Γ.

acceleration due to gravity. A second control parameter is the non-dimensional number fraction $n_\phi = N/N_{max}$, where N is the total number of rods in the container and $N_{max} = (\pi/\sqrt{12})(D/d)^2$ is the maximum number of rods required to obtain a vertically aligned monolayer. Therefore, $n_\phi = 1$ corresponds to having one layer of triangularly packed vertical rods.

III. OBSERVED PATTERNS

The system is initialized by pouring the rods into the container and then increasing Γ, which establishes a random state. Figure 1 shows the phase diagram of the observed patterns as a function of n_ϕ ($f=50$ Hz). The rods are observed to remain static in the initial configuration until $\Gamma \geqslant 1.47$. As Γ is increased above this value, the rods heap towards one side of the container similar to previous observations with spherical particles [12]. As the acceleration is increased further above $\Gamma = 2.6$, the rods are observed to spread out evenly inside the container, and form horizontal layers with random orientations. An example of such a nematic phase observed at low n_ϕ is shown in Fig. 2(a). Above a critical n_ϕ, a second transition is observed. Chaotically moving domains of almost vertical rods are observed to spontaneously form and coexist with horizontal rods [13]. An example is shown in Fig. 2(b).

As n_ϕ is increased further, the domains of near-vertical rods that are formed coalesce and undergo *vortex motion*. Figure 2(c) shows an example of two counterrotating vortices. For large number fractions ($n_\phi > 0.49$), a single large stable vortex made entirely of near-vertical rods in the center and inclined rods at its' boundary is observed [Fig. 2(d)].

If the acceleration is increased further, a gaslike state is reached where the rods vibrate vigorously inside the container and the nematic and vortex states are destroyed. For the highest n_ϕ, a pure gaseous state is not reached due to the limits of the apparatus. Instead, domains of ordered vertical rods are observed to coexist with the gas of rods.

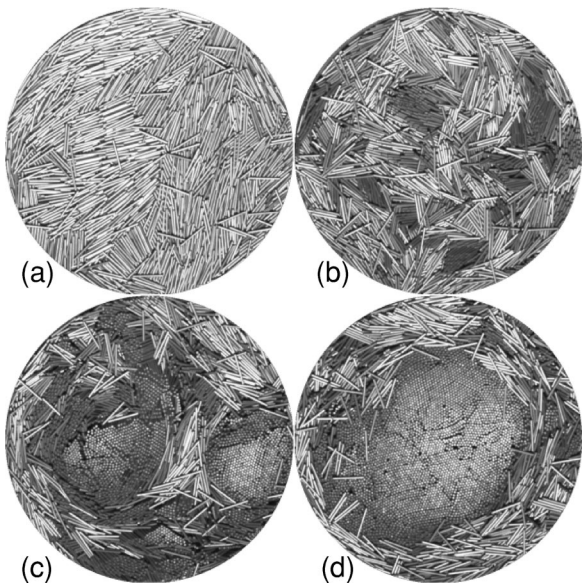

FIG. 2. Examples of patterns observed when granular rods are vertically vibrated ($f=50$ Hz). (a) Nematiclike state ($n_\phi = 0.152$, $\Gamma = 2.42$). (b) Moving domains of near vertical rods ($n_\phi = 0.344$, $\Gamma = 3.38$). (c) Multiple vortices ($n_\phi = 0.551$, $\Gamma = 3.29$). (d) Large vortex ($n_\phi = 0.535$, $\Gamma = 3.00$). The cylindrical surface of the rods is coated with a gray tin-oxide layer to diminish light reflection and has a coefficient of friction $\mu = 0.32$. The patterns that form are imaged from above using a high-frame rate digital camera (Kodak SR-1000). Since the tips of the rods reflect light better than the sides, they appear as bright spots when imaged from above. If the rods are inclined greater than 35°, they reflect far less light compared to nearly vertical and horizontal rods.

A. Domain growth

We now discuss how vortices nucleate and grow as a function of time. An example of the growth process is shown in Fig. 3, and a movie can be viewed at Ref. [14]. Starting from a random state, pockets of near-vertical domains are observed to nucleate uniformly inside the container. This is in contrast with previous observations where the ordered domains grow inward from the boundary [6]. The pockets of vertical domains grow in time by merging to form larger domains of almost vertical rods. The domains are then observed to collectively move as the the system becomes more ordered and then finally show vorticity.

We measure the growth of the domains by taking time-lapse images of the process described above. The growth of near-vertical domains is then measured from the ratio of the domain area to that of the total container area as a function of time. The fraction of rods that are near-vertical, n_v is plotted in Fig. 4 for a range of n_ϕ at a fixed driving acceleration and frequency, $\Gamma = 3.4$ and $f = 50$ Hz.

We find that there exist two growth regimes (a model is discussed in Sec. V). For short times, the growth rate depends on n_ϕ in the following way. If n_ϕ is below a critical value, domains appear but never organize into large vortices. However, as n_ϕ is increased the short time growth is slowed by the high packing. That is, more time is required for small domains to form due to the lack of *voids* present. A void

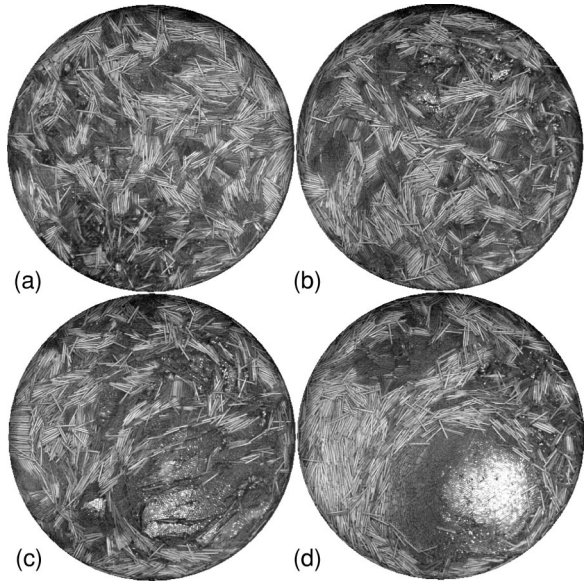

FIG. 3. The formation of the vortex from an initial random state as function of time t of vibration with $\Gamma=2.6$ and $n_\phi=0.39$. (a) $t=3$ min, (b) $t=6$ min, (c) $t=9$ min, (d) $t=12$ min. Small domains of vertical rods are observed to form and coarsen over time and evolve into a vortex ($f=$ 60 Hz).

filling model for domain growth will be discussed in Sec. V. The saturation value of n_v increases with n_ϕ. The difference in the values arises due to the definitions of n_v and n_ϕ.

The variation of the relative number of near-vertical rods as a function of n_ϕ is plotted in Fig. 5. We show separate

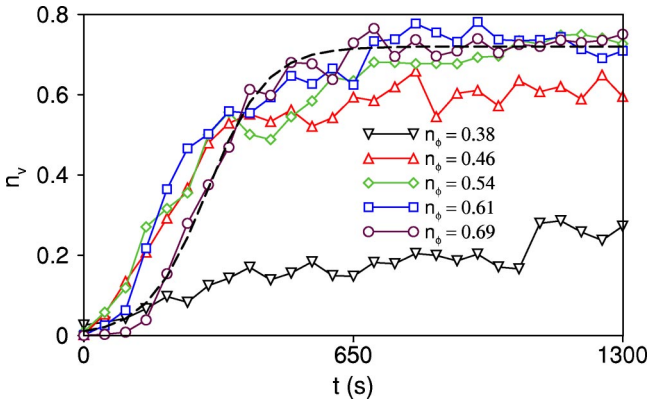

FIG. 4. (Color online) The fraction of vertical rods n_v as a function of time for various n_ϕ at $\Gamma=3.4$ and $f=50$ Hz. The vertical domains show two distinct growth regimes. At short times, the growth is increasing exponentially and then gives way to an exponential decrease in growth to a saturation value determined by n_ϕ. For $n_\phi=0.38$, the domain growth saturates very slowly to a value less than n_ϕ because the near vertical domains cannot be supported by the horizontal rods. For $n_\phi \geq 0.46$ the two distinct growth regimes are apparent and for all n_ϕ vortex motion occurs after $t=300$ s. We note that for the highest value of n_ϕ the initial growth displays a slow down, which is directly related to the void filling mechanism discussed in the text. The dashed line is a fit to the integrated growth equation discussed in Sec. V. We find that the simplified model gives an accurate interpretation of the results.

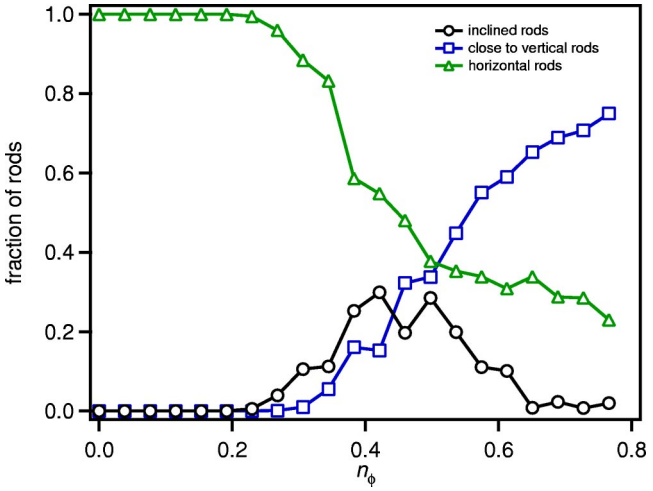

FIG. 5. (Color online) The relative number of inclined, vertical, and horizontal rods as a function of n_ϕ after steady state is reached $\Gamma=3.00$ and $f=50$ Hz.

data for the relative number of inclined rods, vertical rods and horizontal rods. Rods that are tilted between 30° and 80° are considered inclined, and the rest are considered as either horizontal or vertical (the inclination of the rod was obtained by measuring the distance x between adjacent rods and calculating $\sin^{-1}[d/x]$). For $n_\phi<0.22$, the container has only horizontal rods. As n_ϕ increases, more rods tend to the vertical direction. For $n_\phi>0.71$ most rods are either vertical or horizontal.

B. Spatial structure of the vortex and velocity fields

We next discuss the spatial structure of the vortex. In Fig. 6 a close-up image of a vortex pattern is displayed which shows the progressive inclination of the rods from the center of the vortex. We note that the direction of motion corresponds to the direction of inclination (for Fig. 6 the motion is counterclockwise). In this case the inclination of the rods varies from approximately 85° to 40° near the edges. The

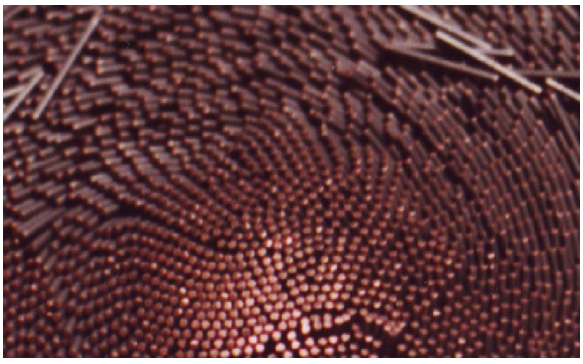

FIG. 6. (Color online) Close-up image of a vortex that has self-organized at $n_\phi=0.419$ (only the upper half of the vortex is shown). The rods are inclined in the direction of rotation, which is counterclockwise. The inclination angle of the rods varies from about 90° at the center of the vortex to near 40° close to the edge.

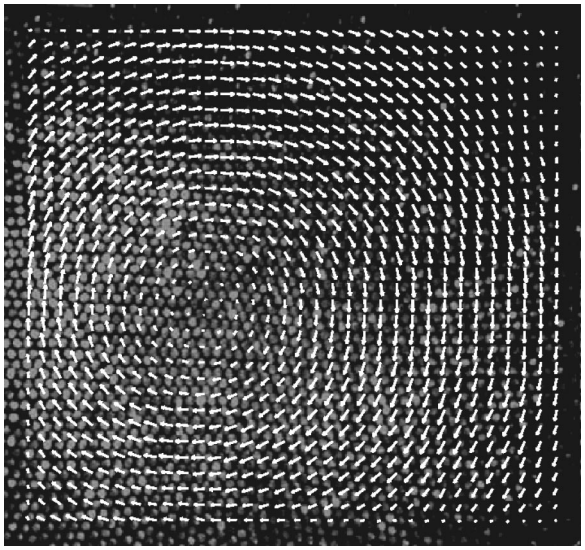

FIG. 7. The velocity field of a granular vortex ($n_\phi = 0.497$, $\Gamma = 3.00$). The data were obtained by tracking individual rod ends and then by spatial and time averaging the obtained displacements (see text).

change in inclination of the rods within the vortex is less at higher n_ϕ due to the increased packing.

By acquiring images at 250 (frames s^{-1}), we were able to track the ends of the vertical rods and obtain the velocity fields of the vortices. In addition to the rotational motion, rods also vibrated due to the collisonal interactions with their neighbors. We first track [15] the ends of the near-vertical rods and then perform spatial and temporal averaging to obtain the vortex fields. An example of the velocity field of a vortex is presented in Fig. 7 (here the temporal averages include 100 consecutive frames, and spatial averages were taken over an area of $2d \times 2d$).

The averaged azimuthal velocity $v(r)$, as a function of the distance r from the center of the vortex, is shown in Fig. 8(a) for a range of n_ϕ. The data was obtained at a constant acceleration $\Gamma = 3.00$ for a frequency $f = 50$ Hz. We note that for small distances relative to the center of the vortices, the averaged velocity $v(r)$ increases linearly with the distance r indicating solid body rotation. At intermediate ranges, this linear relationship is not observed, and therefore shearing occurs inside the vortices. As the boundary of the vortex is approached, velocity decreases due to friction with the horizontal rods at the edge. It is interesting to note that the horizontal rods at the edge of the vortex are often aligned tangentially with the boundary of the vortex [see Fig. 2(c)]. We also observe that the slope of the averaged velocity $v(r)$ at small r systematically decreases as the packing fraction n_ϕ is increased. Thus the angular velocity of the inner core of the vortex decreases with its size.

C. Frequency dependence

We also explored the rotation rate dependence of the vortices as a function of f. Figure 8(b) shows $v(r)$ for $n_\phi = 0.53$ and $\Gamma = 3.00$ for vortices of equivalent size. As stated,

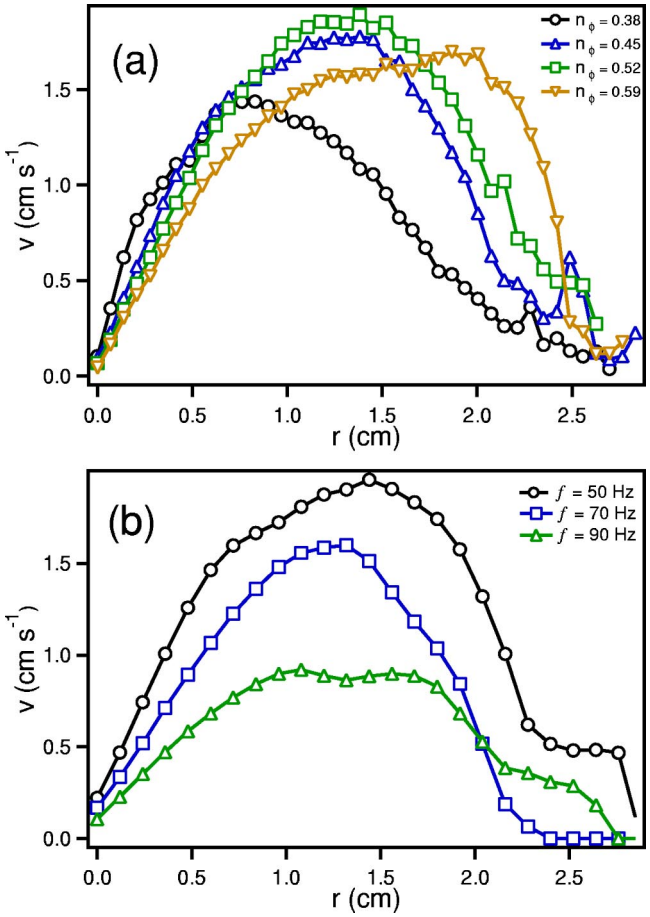

FIG. 8. (Color online) (a) The azimuthal averaged velocity $v(r)$ as a function of the distance r from the center of the vortex. The velocity is observed to increase linearly from the center of the vortex and then reach a maxima before decreasing to the edge of the vortex. The rate of increase of velocity at the center is observed to systematically decrease with n_ϕ and hence vortex size. (b) $v(r)$ as function of frequency f for a fixed Γ at $n_\phi = 0.53$. The velocity of rotation is observed to depend on the velocity of the vibration. $\Gamma = 3.00$ for all data shown.

Γ is held constant while frequency is increased, which decreases vibration velocity. Therefore, we demonstrate that the vortex speed systematically increases with vibration velocity.

IV. HORIZONTALLY VIBRATED CONTAINER

To test if the transition to a vertical state is dependent on the way the container is vibrated, experiments were performed with *horizontal* driving. There do in fact exist similarities: at low n_ϕ heaping and nematiclike domains of horizontal rods are observed; at high n_ϕ the rods tend to align vertically and form ordered domains. An image is shown in Fig. 9. In contrast to the vertical shaking the vertically aligned domains do not migrate and coarsen into vortices. We also find that in this case the convection is stronger and destroys the motion of the vertically ordered domains.

FIG. 9. Image of domains of vertical rods formed when the container is vibrated horizontally. We note that vortices are not observed. The direction of vibration is from left to right. $\Gamma = 1.04$, $f = 30$ Hz, and $n_\phi = 0.612$.

V. DISCUSSION

We first discuss possible mechanisms responsible for the rod to align vertically at high packing fractions. The tendency of the rods to align vertically at high packing fractions may be understood in terms of a void filling mechanism. If voids (i.e., space between rods) are small then they can only be filled with a near-vertical rod. On the other hand, larger voids will accommodate a horizontal rod. Assuming that the distribution of voids decreases with void size, the most probable configuration will be regions of vertical rods. Furthermore, the decrease in the number of large voids is enhanced by the coalescence of regions of vertically aligned rods. This also drives the system to pack more closely and produces a decreased overall center of mass. Thus ordering at high packing fractions can be explained by a process that is analogous to configurational entropy driven ordering in thermal systems [5].

To describe the nucleation and growth of the vertical domains at high n_ϕ shown in Figs. 3 and 4 we present a simple analysis. The rods are assumed to be either vertical or horizontal. We then assume that the growth rate is initially linear and asymptotically must decrease to zero as the number of horizontal rods is diminished and a steady state is reached. Then the evolution of n_v is described by

$$\frac{\partial n_v}{\partial t} = \alpha n_v(\beta - n_v), \tag{1}$$

where α and β are constants that depend on n_ϕ. Equation (1) can be integrated and is fit to the measured $n_v(t)$ in Fig. 4. This simplified interpretation seems to capture the nucleation, growth, and saturation of the near-vertical domains in our experiments.

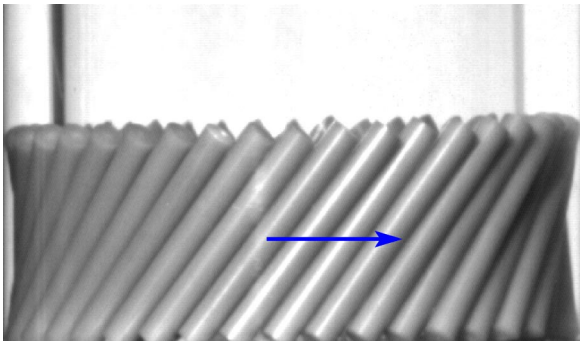

FIG. 10. Image of rods contained in a vertically vibrated 1D annulus. The rods are always observed to move in the direction of inclination. See the text and Ref. [14] for more details.

In previous work by Villarruel *et al.* [6] the experiments were carried out in a system where the diameter of the container and the length of the rods were comparable. The container was tapped and thus the rods experienced considerable shearing with the side boundary. They observed that vertical domains nucleated at the boundaries and subsequently propagate to the center of the cell. These observations are consistent with our findings. We have shown that vertical domains can nucleate away from the sidewalls and form independent of the direction of the driving.

Next, we elucidate the physical mechanism that is responsible for the vortex motion. We performed additional experiments with a row of cylindrical rods with $l = 5.1$ cm and $d = 0.6$ cm in a one-dimensional $1D$ annulus with a mean radius of 5.5 cm (see Fig. 10). When subjected to vertical motion, the rods were always observed to move in the direction of the inclination. No translation motion is observed when the rods were vertical. A movie showing this property can be found at Ref. [14]. We also used ball point pens and pencils to check that the detailed shape of the rod and the tip is not important to this translation mechanism. We find that the translation speed depends on the driving frequency and the inclination is qualitatively similar to that observed for the vortices.

The physical mechanism for the motion of the inclined rods, based on our observation, appears to be as follows. When the inclined rods are vibrated vertically, they hit the bottom plate at a point away from their center of mass. Because the rotation of the rod about its center of mass is constrained due to the neighboring rods, it gets launched in the direction of the inclination. Thus, the greater the inclination of the rods, the further they get launched and land (viz., projectile motion), giving rise to translational motion.

From these direct observations we conclude that the inclined rods form the engine that drives the vortex. The vertical rods in the center of the vortex are simply pulled around by shear induced by the inclined rods. As the number of rods is increased and the size of the vortex increases, the inclination of the rods also decreases because of greater packing. Therefore, the speed of the very large vortices is expected to decrease with the size of the vortex, consistent with our observation [see Fig. 8(a)]. We also note that the frequency dependence of $v(r)$ is compatible with the mechanism de-

scribed above. By decreasing the frequency of the driving signal at fixed Γ the velocity of the driving plate is increased. Therefore, one expects $v(r)$ to increase with a decrease in frequency, consistent with our observations [see Fig. 8(b)].

VI. CONCLUSION

In conclusion, granular rods are observed to form vertically aligned domains at high packing fractions, independent of the direction of vibration. Vortex patterns are observed when the rods are vibrated vertically. We have measured the growth of near-vertical domains and have developed a simple *void filling* model that well describes our results. We have also shown a new translation mechanism which occurs due to anisotropy. Based on these observations, Aranson and Tsimring [16] have developed a phenomenological model that describes the formation and coarsening of the vortices.

ACKNOWLEDGMENTS

We acknowledge stimulating discussions with Lev Tsimring and Igor Aranson, and Eric Frederick for assistance with the experiments. We thank Seth Fraden for inspiring the experiments, for sharing unpublished data, and for providing us with some of the rods which were purchased under his NSF grant, DMR-0088008. This work was supported by the NSF under Grant No. DMR-9983659, and by the donors of the Petroleum Research Fund.

[1] F. Melo, P. B. Umbanhowar, and H. L. Swinney, Phys. Rev. Lett. **72**, 172 (1994); **75**, 3838 (1995).
[2] J. B. Knight, H. M. Jaeger, and S. R. Nagel, Phys. Rev. Lett. **70**, 3728 (1993).
[3] S. G. K. Tennakoon, and R. P. Behringer, Phys. Rev. Lett. **81**, 794 (1998).
[4] H. A. Makse, S. Havlin, P. R. King, and H. E. Stanley, Nature (London) **386**, 379 (1997).
[5] C. C. Mounfield and S. F. Edwards, Physica A **210**, 279 (1994).
[6] F. X. Villarruel, B. E. Lauderdale, D. M. Mueth, and H. M. Jaeger, Phys. Rev. E **61**, 6914 (2000).
[7] L. Onsager, Ann. N.Y. Acad. Sci. **51**, 627 (1949).
[8] V. A. Baulin and A. R. Khokhlov, Phys. Rev. E **60**, 2973 (1999); B. J. Buchalter, and R. M. Bradley, Europhys. Lett. **26**, 159 (1994).
[9] Z. Dogic and S. Fraden, Phys. Rev. Lett. **78**, 2417 (1997).
[10] F. M. van der Kooij, K. Kassapidou, and H. N. W. Lekkerkerker, Nature (London) **406**, 868 (2000).
[11] P. G. de Gennes, and J. Prost, *The Physics of Liquid Crystals*, 2nd ed. (Oxford Science, New York, 1993).
[12] P. Evesque and J. Rajchenbach, Phys. Rev. Lett. **62**, 44 (1989).
[13] S. Fraden (private communication).
[14] See EPAPS Document No. E-PLEEE8-67-161303 for movies showing the vorticity of the patterns (also available at http://physics.clarku.edu/vortex). A direct link to this document may be found in the online article's HTML reference section. The document may also be reached via the EPAPS homepage (http://www.aip.org/pubservs/epaps.html) or from ftp.aip.org in the directory /epaps/. See the EPAPS homepage for more information.
[15] J. C. Crocker and D. G. Grier, J. Colloid Interface Sci. **179**, 298 (1996).
[16] I. S. Aranson and L. S. Tsimring, e-print cond-mat/0203237.